Criterion for Sufficiently Large Dither Amplitude to Mitigate Non-linear Glitches

Ahmad Faza', John Leth, and Arnfinn A. Eielsen

Abstract— **A model describing glitch disturbances is introduced and analysed. The model is used to find the response of glitch disturbances when adding a periodic dither to the input and applying low-pass filtering to the output. This averaged response is used to find a criterion to determine a sufficiently large dither amplitude that will make the averaged glitch disturbances appear as a constant on the output of the low-pass filter. An important resulting property is that the averaged response to glitch disturbances is independent of the model input. By fitting the model to the measured response of a common off-the-shelf digital-to-analogue converter, simulations are used to verify the analytical results.**

I. INTRODUCTION

Glitches can be described as unwanted, transient disturbances of short duration, often resembling spikes in a waveform. As such, they are known to occur in e.g. multilevel power converters [1]–[3], systems with friction [4,5] and in digital-to-analogue converters [6]–[9]. In this paper, a glitch model is developed and analysed and applied and fitted to the response seen in a digital-to-analogue converter (DAC).

For DACs, glitches are typically caused by timing mismatches for transistor switching [6]–[9] and is a deterministic effect generated when a DAC switches between two output levels. Specifically, a glitch occurs when the analogue signal value corresponding to a given digital code appears before or after the signal value of the previous code disappears at the DAC output. The glitch properties of a DAC are often specified by the net area of the glitch impulse response [10] or sometimes by the area at the worst-case code transition [11]. Fig. 1 illustrates deviations from ideal operation common in conventional DACs. The diagram shows the effects of a static non-linearity known as element mismatch or integral non-linearity (INL), as well as glitches of different severity. It should be noted that some non-ideal effects in DACs, including INL, can effectively be mitigated when the DAC is part of a closed-loop system. However, glitches will not be mitigated due to their wide-bandwidth, impulse-like behaviour, where most of the power in the disturbance is outside the bandwidth of the control law.

Dither is a well-known method for static non-linear effects mitigation, including quantisation [12,13] and element mismatch [14]. Dynamic effects are also known to be mitigated in a similar fashion [4,15]; this effect has been demonstrated specifically for glitches [16]. Dither is a high-frequency periodic or stochastic signal introduced into a system to modify its non-linear characteristics [4,17]–[20]. If sufficient averaging (low-pass filtering) is present on the output of the non-linear element, there is a smoothing effect on the non-linearity, typically making it less pronounced. An advantage of this method is that no specific knowledge of the non-linearity is needed in order to obtain improved performance. Specifically, dithering can easily be retrofitted to existing devices such as DACs, with little effort.

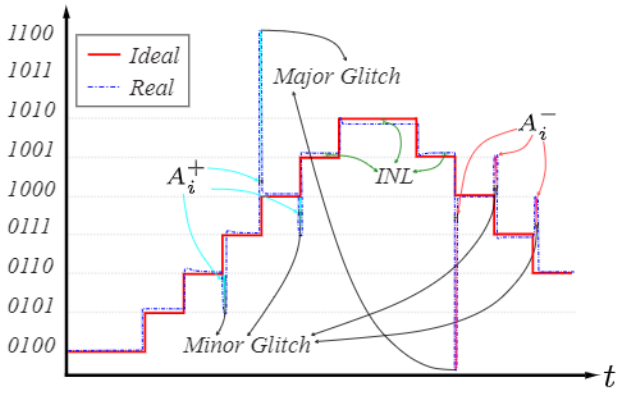

Fig. 1. Persistent non-linear deviations in conventional DACs including INL, and glitches. Where A_i^+ (A_i^-), indicate net areas of impulse responses for glitches due to references of rising (falling) trend.

A. Contributions

Previous investigations utilising large-amplitude, high-frequency periodic dither [16] note that the response of dithered glitches with averaging using a low-pass filter converts the glitches from large-amplitude impulse-like (short duration) disturbances, into small-amplitude, step-like (long duration) disturbances. Exploiting this behaviour combined with feedback control in [21], suggests that a large enough dither amplitude has the potential of almost complete glitch mitigation. This work aims to analytically determine the averaged response of dithered glitches due to the injection of large-amplitude, high-frequency periodic dither. A survey of existing glitch models can be found in [16], as well as a novel model for symmetric and asymmetric glitches that is amenable to mathematical analysis. Glitch response bounds are provided for the two types of glitches when excited by stochastic or periodic dithers. In this paper, a simplified glitch model is developed; it still predicts the most salient effects caused by glitches, but enables the development of an analytical criterion for determining a sufficiently large dither amplitude for complete glitch mitigation.

Ahmad Faza' (ahmad.faza@uis.no), Arnfinn A. Eielsen (eielsen@ux.uis.no) are with the Dept. of Energy and Petroleum Engineering, University of Stavanger, Norway

J. Leth (jjl@es.aau.dk) is with the Dept. of Electronic Systems, Automation & Control, Aalborg University, Denmark

B. Notation

In this paper we generally assume that signals are functions of the following type

$$\mathbb{R}_{\geq 0} \to [X_{min}, X_{max}];\ t \mapsto x(t).$$

When there is no chance of misunderstanding we often leave out index sets, that is, a statement like $F_i = F_j$ for $i < j$ and all $i, j \in \{1, 2, \ldots, k\}$ would be written simply as $F_i = F_j$ for $i < j$.

II. DITHERING

In general, a (periodic) dither is understood to be any bounded, periodic and sufficiently regular function $p : [0, \infty) \to \mathbb{R}$, e.g. a sinusoidal, square wave or triangular wave signal. In this paper, p is thought of as a periodic high-frequency (HF) signal. Now let $n(w)$ denote any function of bounded variation (e.g. the input-output behaviour of a quantiser, see $Q(w)$ in (23)), then using a ρ-periodic dither signal p we may define the smoothed non-linearity $N(x)$ as

$$N(x) \triangleq \int_{\mathbb{R}} n(x+v)\mathrm{d}F_p(v)\ , \tag{1}$$

where $F_p(v)$ is the amplitude distribution function of p given by $F_p(v) = 1/\rho \cdot \mu\{t \in [0, \rho) \mid p(t) \leq v\}$ where μ is the Lebesgue measure. See [18]–[20] for a detailed mathematical treatment of dither signals. Given that F_p is an absolutely continuous distribution, the averaging effect of the dither p on the non-linearity $n(w)$ is generally found by evaluating the Lebesgue-Stieltjes integral (1) as

$$\int_{\mathbb{R}} n(x+v)\mathrm{d}F_p(v) = \int_{\mathbb{R}} n(x+v) f_p(v)\mathrm{d}v\ , \tag{2}$$

where $f_p(v)$ is the amplitude density function, defined by

$$f_p(v) \triangleq \frac{\mathrm{d}}{\mathrm{d}v} F_p(v)\ . \tag{3}$$

This means the smoothed non-linearity $N(x)$ can be found as the cross-correlation of the function $n(w)$ and the amplitude density function of the dither. The integral (1) is equivalent to the time-average over one period ρ of the periodic dither, where x is assumed to be constant for the duration of the period [20]:

$$\int_{\mathbb{R}} n(x+v)\mathrm{d}F_p(v) = \frac{1}{\rho}\int_0^{\rho} n\left(x + p(t)\right)\mathrm{d}t\ . \tag{4}$$

To make this more precise, in [20] it is shown that when $L_D \triangleq \sup_{z\in\mathbb{R}} |f_d(z)| < \infty$; then for each $\bar{t} \geq 0$ let $J_{\bar{t}} = [\bar{t} - \rho, \bar{t})$ denote the interval of length $\rho > 0$; if $x(t)$ has a Lipschitz constant $L_X = L_X(J_{\bar{t}})$ on $J_{\bar{t}}$ then:

$$\left|\int_{J_t} n(x(\tau) + p(\tau))\,\mathrm{d}\tau - \int_{J_t} n(\tilde{x} + p(\tau))\,\mathrm{d}\tau\right| \leq 2L_D L_X T V(n)\rho^2 \tag{5}$$

where $TV(n)$ is the total variation of $n(u)$, with $\tilde{x}$ satisfying

$$\min_{t\in J_t} x(t) \leq \tilde{x} \leq \max_{t\in J_t} x(t)\,. \tag{6}$$

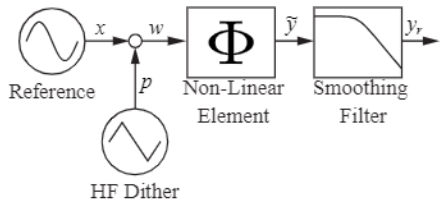

Fig. 2. System block diagram - reference input $x = x(t)$, periodic dither $p = p(t)$, (dithered) input to non-linear element $w = w(t)$, (dithered) non-linear element output $\tilde{y} = \tilde{y}(t)$, averaged output $y_r = y_r(t)$.

Note that from (5), the error due to the assumption of x being piece-wise constant with duration ρ, goes to zero as $\rho \to 0$.

A signal with uniform amplitude density

$$f_p(v) = \frac{1}{2A_d}\mathrm{rect}\left(\frac{v}{2A_d}\right) = \begin{cases} \frac{1}{2A_d} & |v| \leq A_d \\ 0 & |v| > A_d \end{cases}\ , \tag{7}$$

where A_d is the periodic dither amplitude, is an example of a signal with an absolutely continuous amplitude distribution function $F_p(v)$ (with $L_D = \frac{1}{2A_d}$). In this paper, the chosen dither representation is a ρ-periodic triangular wave dither p given by

$$p(t) = \begin{cases} A_d - \frac{4A_d}{\rho}t, & t \in [0, \rho/2] \\ \frac{4A_d}{\rho}(t - \frac{\rho}{2}) - A_d, & t \in [\rho/2, \rho) \end{cases}\ . \tag{8}$$

We assume that for given reference $x(t)$, the period ρ is chosen (sufficiently small) such that $x(t)$ is approximately constant on any time interval of length ρ, i.e. the error (5) is negligible.

III. ANALYTICAL FRAMEWORK

A diagram of the modelled system is shown in Fig. 2. It consists of a non-linear element Φ, and a reconstruction filter.

A. Modeling Glitches

Let $\tilde{y}(t) = \phi(w(t))$ denote the input-output behavior of Φ. We work under the assumption that the effect of glitches is an additive disturbance. That is, we may write $\phi(w(t)) = n(w(t)) + n_g(w(t))$ with $n_g(w(t))$ describing the effect of glitches and $n = \phi - n_g$ accounts for all other effects. We use the following (input-dependent) glitch model

$$n_g(w(t)) \triangleq \sum_{i=1}^{N_T} n_{g_i}(w(t)) \triangleq \sum_{i=1}^{N_T} A_i^{\pm}(w(t))\delta(w(t) - T_i)\,. \tag{9}$$

with δ the Dirac delta function, T_i a threshold value where a glitch is triggered and $T_i = T_j$ only when $i = j$, and N_T the number of glitch transitions T_i. Thus, n_{g_i} describes the glitch related to transition level T_i. The (input-dependent) glitch area $A_i^{\pm}$ is defined as

$$A_i^{\pm}(w(t)) \triangleq \begin{cases} 0 & w(t-\tau) = w(t) \\ A_i^- & w(t-\tau) > w(t) \\ A_i^+ & w(t-\tau) < w(t) \end{cases} \tag{10}$$

with $\tau > 0$ a finite time-delay. Here, the time delay is used to determine if the input is rising or falling, but is in practice determined by, e.g. the sampling time in a device (the non-linear element Φ). For a DAC τ is limited by the duration between two consecutive input writes, typically the inverse of the maximum sample rate. A_i^- are the glitch areas for falling input, and A_i^+ the glitch areas for rising input.

B. Dithered Glitch Response

Now for each glitch n_{g_i} define the smoothed non-linearity $N_i(x)$ by

$$N_i(x) \triangleq \frac{1}{\rho}\int_0^\rho n_{g_i}\left(x + p(t)\right)\mathrm{d}t$$
$$= \frac{1}{\rho}\int_0^\rho A_i^{\pm}(x+p(t))\delta(x+p(t)-T_i)\mathrm{d}t \quad x \in \mathbb{R}. \quad (11)$$

Clearly $N_i(x) \neq 0$ iff $x + p(t) - T_i = 0$. Using (8) we therefore get

$$N_i(x) \neq 0 \quad \text{iff}$$
$$x = \begin{cases} \frac{4A_d}{\rho}t + (T_i - A_d), & t \in [0, \rho/2] \\ -\frac{4A_d}{\rho}t + (T_i + 3A_d), & t \in [\rho/2, \rho) \end{cases}, \quad (12)$$

implying that $x \in [T_i - A_d, T_i + A_d] \triangleq I_x$. To calculate the value $N_i(x)$ (for $x \in I_x$) first note that $A_i^{\pm}(x + p(t)) = A_i^{\pm}(p(t))$, hence we need to find the sign of $p(t) - p(t-\tau)$ at the one or two time instances where $p(t) = T_i - x$ (see Fig. 3 for illustration). Again using (8) we get

$$A_i^{\pm}(p(t_1)) + A_i^{\pm}(p(t_2)) =$$
$$\begin{cases} A_i^+ + A_i^+ & \text{for} \quad A_d > T_i - x > p\left(\frac{\tau}{2}\right) \\ 0 + A_i^+ & \text{for} \quad T_i - x = p\left(\frac{\tau}{2}\right) \\ A_i^- + A_i^+ & \text{for} \quad p\left(\frac{\tau}{2}\right) > T_i - x > p\left(\frac{\tau}{2} + \frac{\rho}{2}\right) \\ A_i^- + 0 & \text{for} \quad T_i - x = p\left(\frac{\tau}{2} + \frac{\rho}{2}\right) \\ A_i^- + A_i^- & \text{for} \quad -A_d < T_i - x < p\left(\frac{\tau}{2} + \frac{\rho}{2}\right) \end{cases}$$

or

$$A_i^{\pm}(p(t_1)) = \begin{cases} A_i^+ & \text{for} \quad T_i - x = A_d \\ A_i^- & \text{for} \quad T_i - x = -A_d \end{cases}$$

and therefore

$$N_i(x) =$$
$$\frac{1}{\rho}\begin{cases} 0 & \text{for} \quad x < T_i - A_d \\ A_i^+ & \text{for} \quad x = T_i - A_d \\ A_i^+ + A_i^+ & \text{for} \quad T_i - A_d < x < T_i - p\left(\frac{\tau}{2}\right) \\ 0 + A_i^+ & \text{for} \quad x = T_i - p\left(\frac{\tau}{2}\right) \\ A_i^- + A_i^+ & \text{for} \quad T_i - p\left(\frac{\tau}{2}\right) < x < T_i - p\left(\frac{\tau}{2} + \frac{\rho}{2}\right) \\ A_i^- + 0 & \text{for} \quad x = T_i - p\left(\frac{\tau}{2} + \frac{\rho}{2}\right) \\ A_i^- + A_i^- & \text{for} \quad T_i + A_d > x > T_i - p\left(\frac{\tau}{2} + \frac{\rho}{2}\right) \\ A_i^- & \text{for} \quad x = T_i + A_d \\ 0 & \text{for} \quad x > T_i + A_d \end{cases} \quad (13)$$

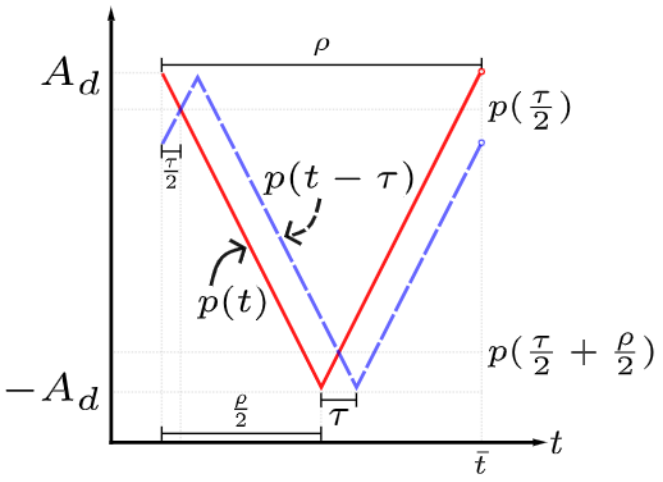

Fig. 3. Illustrating $p(t), p(t-\tau)$: where for a certain level T_i fixed on the vertical axis, x is viewed as a vertical shift to the plots $p(t), p(t-\tau)$.

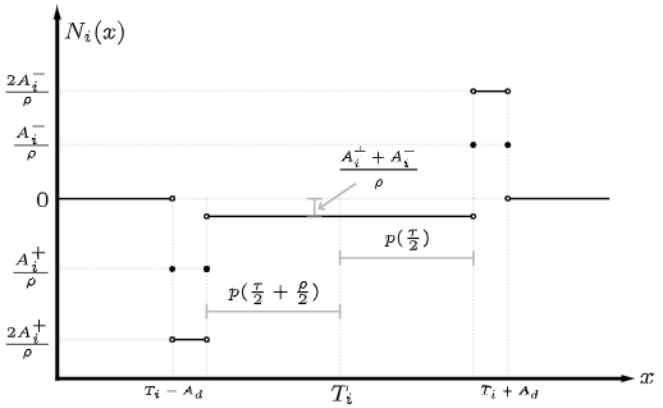

Fig. 4. $N_i(x)$ - the smoothed non-linearity of a single glitch n_{g_i}, due to a periodic dither $p(t)$.

as depicted in Fig. 4. It is remarked that for a given practical DAC implementation, the range of DAC input values $x(t)$ is set depending on the performed operation. Moreover, the thresholds T_i, the accompanying areas A_i^-, A_i^+, and the time-delay τ are the hardware-dependent quantities related to the DAC topology, non-linear deviations from ideal DAC response and time-duration between consecutive write commands, respectively. Hence, the design freedom to obtain a desired $N_i(x)$ for a set range of DAC input values $x(t)$ remains in the choice of the dither signal, which is determined from (8) and (13) by choice of A_d and ρ.

IV. Criteria for Sufficiently Large Dither

A. Choosing the Dither Frequency

The time-delay τ is an implementation-dependent parameter typically determined by the maximum allowable rate for DAC write operations, or maximum sample-rate. We assume that maximising the sample-rate for a specific DAC is beneficial and this is determined by $1/\tau$. The period of the dither ρ can be chosen considering (5) in Sec. II; where the dither should vary at a high rate relative to the reference

input x in order to minimize the error for the piece-wise constant approximation on x over any $J_{\bar{i}}$; i.e., choosing $0 < \tau << \rho$ such that $(x - \tilde{x}) \to 0$ for $\rho \to 0$. Furthermore, since we are analysing the system in continuous time, the sampling rate should be at least 5-10 times higher than the dither frequency in order for the discrepancy between the continuous description and discrete-time description to be small [22]. If the ratio between the sampling frequency and dither frequency becomes too small, discrete-time effects start to dominate and the presented analysis and behaviour of the system become very different. Summarily, the dither frequency should be chosen as high as possible to minimise the approximation error (5), but at least 5-10 times below the sampling-rate to avoid discrete-time artefacts.

The dither frequency is constrained by the possible sampling rate, and the effect of the dither is then determined by the amplitude A_d.

B. Criterion I: Single Glitch

It is evident from (9) that $n_{g_i}(x(t))$ only depends on $x(t)$ when T_i is in the range of $x(t)$, that is, when $T_i \in [X_{\min}, X_{\max}]$. Note from (13) that A_d affects the width of the various sectors in Fig. 4. The sector heights are determined by implementation-dependent parameters. The width of the sector where $N_i(x) = (A_i^- + A_i^+)/\rho$ for $x \in (T_i - p(\tau/2), T_i - p(\tau/2 + \rho/2))$ can be adjusted by varying A_d. The goal is to suppress the effect of $n_{g_i}(x(t))$. The smooth image $N_i(x(t))$ cannot be made null for any choice of A_d unless A_i^-, A_i^+ are null, or $A_i^- + A_i^+ = 0$. In practice, it is more likely for $A_i^- + A_i^+$ to be closer to zero than either A_i^- or A_i^+; i.e. A_i^-, A_i^+ have opposing signs. Hence, A_d can be chosen such that $N_i(x) = (A_i^- + A_i^+)/\rho$ for $x \in [X_{\min}, X_{\max}]$, which implies that $N_i(x(t)) = (A_i^- + A_i^+)/\rho$ for $t \geq 0$.

A sufficiently large dither amplitude A_d is defined as one such that $N_i(x(t))$ is constant. A constant $N_i(x(t))$, independent of the DAC input, can then be removed if the DAC is operating in closed-loop or by an offset correction circuit if operated in open-loop. A sufficiently large dither amplitude A_d is determined using (13) and (8); $N_i(x) = (A_i^- + A_i^+)/\rho$ when

$$\begin{aligned} &T_i - p\left(\frac{\tau}{2}\right) < x < T_i - p\left(\frac{\tau}{2} + \frac{\rho}{2}\right) \\ &\quad \Rightarrow -A_d\left(1 - \frac{2\tau}{\rho}\right) < T_i - x < A_d\left(1 - \frac{2\tau}{\rho}\right) \end{aligned} \quad (14)$$

and the averaged non-linearity $N_i(x) = (A_i^- + A_i^+)/\rho$ for all $A_d > \rho/(\rho - 2\tau)\,|T_i - x|$. Extending this to a range of x values, A_d is a sufficiently large dither amplitude for all $x \in [X_{\min}, X_{\max}]$ if

$$A_d > \left(\frac{\rho}{\rho - 2\tau}\right) \max\{|T_i - X_{\min}|, |T_i - X_{\max}|\}. \quad (15)$$

C. Criterion II: Several Equidistant Glitches

Since glitch thresholds correspond to quantisation levels in DACs, consecutive glitch thresholds are treated to be equidistant; i.e., $T_i - T_{i-1} = \Delta T$. Equidistant glitches can, as in Sec. IV-B, be minimized in the same sense by choosing a sufficiently large dither amplitude A_d. Note that for $A_d \geq \Delta T/2$ there will be an overlap between $N_i(x), N_{i-1}(x)$, meaning that the proposed criteria in (15) would only render $N_g(x)$ constant for all $x \in [X_{\min}, X_{\max}]$ when $[X_{\min}, X_{\max}] \subseteq [T_i - (\rho - 2\tau)\Delta T/2\rho, T_i + (\rho - 2\tau)\Delta T/2\rho]$. An alternative trivial solution would be to take

$$\max_{j \in \{1,2,3,\ldots N_T\}} \{A_d(j)\} \quad (16)$$

where

$$A_d(j) = \left(\frac{\rho}{\rho - 2\tau}\right) \max\{|T_j - X_{\min}|, |T_j - X_{\max}|\}. \quad (17)$$

This is undesirable as $p(t)$ will occupy the entire permissible input range; i.e., $x(t) + p(t)$ will exceed the DAC input limits for any non-zero $x(t)$. Note the special case for when $A_{j-1}^{\pm} = A_j^{\pm} = A_{j+1}^{\pm}$, we have $N_i(x) = N_j(x + (j - i)\Delta T)$ for $j > i$. By this property, choosing $A_d : T_i - p(\tau/2) = T_{i-1} + A_d$ and $T_i - p(\tau/2 + \rho/2) = T_{i+1} - A_d$ will join the sectors of neighbouring N_i such that N_g is almost constant over the entire allowable range of inputs:

$$\begin{aligned} p\left(\frac{\tau}{2}\right) + A_d = T_i - T_{i-1} = T_{i+1} - T_i = A_d - p\left(\frac{\tau}{2} + \frac{\rho}{2}\right) \\ \Rightarrow \Delta T = 2A_d\left(1 - \frac{\tau}{\rho}\right) \end{aligned} \quad (18)$$

Therefore,

$$A_d = \left(\frac{\rho}{\rho - \tau}\right)\frac{\Delta T}{2}. \quad (19)$$

The choice of A_d as in (19) results an averaged non-linearity N_g of several equidistant glitches $n_g(x)$ as follows (with $A^+ = A_i^+$ and $A^- = A_i^-$):

$$N_g(x) = \frac{1}{\rho}\begin{cases} 0 & \text{for} \quad x < T_1 - A_d \\ A^+ & \text{for} \quad x = T_1 - A_d \\ A^+ + A^+ & \text{for} \quad T_1 - A_d < x < T_1 - p(\frac{\tau}{2}) \\ 0 + A^+ & \text{for} \quad x = T_1 - p(\frac{\tau}{2}) \\ \\ 2(A^- + A^+) & \text{for} \quad T_{i-1} - A_d < x < T_{i-2} + A_d \\ A^- + A^+ & \text{for} \quad T_{i-2} + A_d \leq x \leq T_i - A_d \\ 2(A^- + A^+) & \text{for} \quad T_i - A_d < x < T_{i-1} + A_d \\ A^- + A^+ & \text{for} \quad T_{i-1} + A_d \leq x \leq T_{i+1} - A_d \\ 2(A^- + A^+) & \text{for} \quad T_{i+1} - A_d < x < T_i + A_d \\ A^- + A^+ & \text{for} \quad T_i + A_d \leq x \leq T_{i+2} - A_d \\ 2(A^- + A^+) & \text{for} \quad T_{i+2} - A_d < x < T_{i+1} + A_d \\ \\ A^- + 0 & \text{for} \quad x = T_{N_T} - p(\frac{\tau}{2} + \frac{\rho}{2}) \\ A^- + A^- & \text{for} \quad T_{N_T} + A_d > x > T_{N_T} - p(\frac{\tau}{2} + \frac{\rho}{2}) \\ A^- & \text{for} \quad x = T_{N_T} + A_d \\ 0 & \text{for} \quad x > T_{N_T} + A_d \end{cases} \quad (20)$$

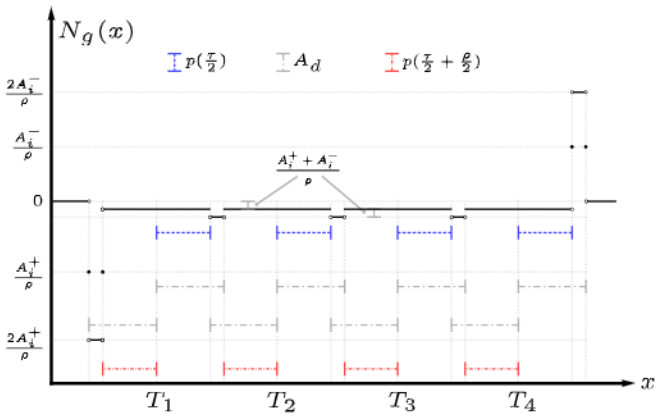

Fig. 5. $N_g(x)$ - the smoothed non-linearity of the total glitch n_g for $N_T = 4$, due to a periodic dither $p(t)$ of sufficiently large amplitude from (19).

Fig. 5 illustrates an example of N_g following (20) for n_g as a sum of 4 ($N_T = 4$) equidistant glitches of identical (input-dependent) glitch areas $A_i^{\pm}$.

V. VERIFICATION MODEL

The non-linear DAC model in [21], is used to verify the analysis in Sec. III. The model is an instance of the non-linear element Φ in Fig. 2. The model parameters are fitted to the measured response of a commercial 16-bit DAC; the Texas Instruments DAC8544. The model includes quantisation error q and element mismatch n_{em}, as experimentally validated in [14], and glitches n_g as experimentally validated in [16]. The model response describes the measured response to a high degree [14,16].

A. Modelling the DAC

1) Uniform Quantization: A DAC has 2^B levels, where B is the word size (bits). The quantization step size is

$$\delta = \frac{\Delta}{2^B - 1}\,, \tag{21}$$

where Δ is the physical output range of the DAC. A mid-tread uniform quantizer is defined using the truncation operator $T(w)$

$$k = T(w) = \left\lfloor \frac{w}{\delta} + \frac{1}{2} \right\rfloor\,, \tag{22}$$

where $\lfloor\cdot\rfloor$ denotes the floor operator and w the input which typically is dependent on time t, that is, $w = w(t)$. The truncation operator is a discontinuous function. The output y of the quantizer given an input w is

$$y = Q(w) = \delta T(w) = \delta k\,. \tag{23}$$

The quantization error $q(w)$ is defined as the function

$$q(w) \triangleq y - w = Q(w) - w\,. \tag{24}$$

The output can then be modeled as:

$$y = w + q(w)\,. \tag{25}$$

2) Modelling Glitches: The glitch model proposed in [16], constructs glitches as short, symmetric or asymmetric rectangular pulses with unit areas driving a linear-time invariant (LTI) filter. The pulse response of the LTI filter can be designed to approximate any glitch shape. Symmetric glitches n_{g_s} have an input-dependent polarity; where glitch polarity is determined by how the DAC input signal crosses threshold values where glitch transitions occur (i.e. rising or falling) while glitch amplitudes remain symmetric in both directions. For asymmetric glitches $n_{g_{\bar{s}}}$ both the glitch polarity and amplitude depend on whether the DAC input is falling or rising; i.e. rising glitch transitions may have different polarity and amplitude than falling glitch transitions. A symmetric glitch is modelled as

$$n_{g_s}(w(t)) \triangleq \sum_{i=1}^{N_{T_s}} \left(g_i * \Delta y_i\right)(t)\,, \tag{26}$$

where $*$ denotes convolution, N_{T_s} is the number of marginal symmetric glitch transitions occurring at each least-significant bit (LSB), g_i is a linear time-invariant (LTI) filter impulse response determining the shape of glitch i and

$$\Delta y_i(t) = \frac{1}{\tau}(H(Q(w(t)) - T_i) - H(Q(w(t-\tau_i)) - T_i))$$

with $H(\cdot)$ the Heaviside step-function, T_i a threshold value where a glitch is triggered and $T_i = T_j$ only when $i = j$. The time-delay $\tau_i > 0$ defines the glitch width and height (here τ_i is chosen such that $\tau = \tau_i = \tau_j$ for all i, j; which means unit-area rectangular pulses).

For Texas Instruments DAC8544 the major asymmetric glitch transitions $N_{T_{\bar{s}}}$ occur at code intervals of 4096; i.e. 16 glitch thresholds in total. For the more general asymmetric glitch model $n_{g_{\bar{s}}}$ see [16].

3) Complete Non-linear DAC Model: Element mismatch n_{em} is modelled as an additive static non-linearity given by

$$n_{em} = \delta \mathrm{INL}(w)\,, \tag{27}$$

where the static non-linear function $\mathrm{INL}(w)$ is called the integral non-linearity [8,14] defined by

$$\mathrm{INL}(w) \triangleq \frac{\tilde{y}(w) - \delta T(w)}{\delta}\,, \tag{28}$$

where $\tilde{y}(w)$ are measured DAC output values corresponding to an input value w obtained to reflect DAC output deviation from the ideal quantization value (23) due to element mismatch (without accounting for glitches). From (28) we therefore get the following DAC output model

$$\tilde{y}(w) = y(w) + \delta \mathrm{INL}(w)\,. \tag{29}$$

To incorporate the effect of glitches into the non-linear DAC model, the dynamic non-linearity n_g is introduced. Let $n_g \triangleq n_{g_s} + n_{g_{\bar{s}}}$ denote the effect of the symmetric and asymmetric glitches [16], the DAC output (29) can then be modified by the following DAC output model:

$$\tilde{y}(w(t)) = y(w(t)) + n_{em}(w(t)) + n_g(w(t)) \tag{30}$$

A diagram of the non-linear quantiser is shown in Fig. 6.

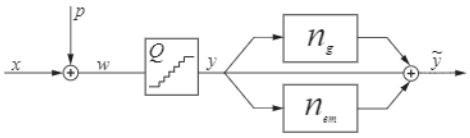

Fig. 6. Non-linear DAC model [21].

B. Reconstruction Filter

The smoothing filter in Fig. 2 is implemented as a fourth-order filter (two cascaded Butterworth filters) with transfer-function $W_r(s)$. A reconstruction or smoothing filter is required to reduce repeated spectra due to sampling and also reduces quantisation effects. These filters are usually designed to attenuate frequency content above the Nyquist-frequency. In terms of averaging non-linear effects by dithering, the filter is a practical implementation of the time-average on the right-hand side of (4). To increase the averaging effect the cut-off frequency should be chosen significantly lower than the Nyquist-frequency. Note that retrofitting dither to a conventional application requires minimal changes since averaging is achieved using an existing component. $W_r(s)$ has the form

$$W_r(s) = \left(\frac{{\omega_c}^2}{s^2 + \sqrt{2}\omega_c s + {\omega_c}^2} \right)^2 , \qquad (31)$$

where ω_c is the cut-off frequency in rad/s.

VI. RESULTS AND DISCUSSION

The models used for analysis and for verification are different; the analysis model in Sec. III-A is a simplification capturing the most salient response and enabling analytical results, whilst the verification model in Sec. V-A.2 behaves more in accordance with physical implementation. The two models are related via the net areas A_i^+, A_i^- for a given threshold T_i. For the model fitted to the Texas Instruments DAC8544 response, $N_T = 2^{16} - 1 = (N_{T_s} + N_{T_{\tilde{s}}})$ and T_i represents the quantisation levels. Symmetric glitches in Sec. V-A.2 is a special case of asymmetric glitches when $A_j^+ = -A_j^-$. Both symmetric (minor) and asymmetric (major) glitches are described by the values T_i, A_i^+, A_i^- for each glitch in (9) and (10).

For the verification model the parameter τ also determines the glitch duration. For the majority of DACs this would most accurately be set equal to the duration of a write operation (i.e. the inverse of the maximum sample-rate). The glitch energy is delivered within this duration; $A_i^{(+/-)} = (A_i^{(+/-)}/\tau) \cdot \tau$.

A. Simulations

The full-scale range (FSR) of the Texas Instruments DAC8544 is ± 5 V. A least significant bit (LSB) is therefore $\delta = 10/(2^{16} - 1)$ V. The 16 areas for the major (asymmetric) glitches (equidistant with $\Delta T_{\tilde{s}} = 4096$ LSB) were measured to be $A_j^+ = -60.6$ nVs for rising input, and $A_j^- = 51.9$ nVs for falling input. The $2^{16} - 16$ areas of the minor (symmetric) glitches (equidistant with $\Delta T_s = 1$ LSB) were measured to be $A_j^+ = -A_j^- = \pm 2.40$ nVs. The glitch duration was set to $\tau = 1\,\mu$s matching the inverse of the maximum sample-rate for the DAC. As no additional dynamic effects were included in the modelling, the simulation time step was set equal to the inverse of the maximum sample-rate; i.e., $f_s = 1$ MHz. For a given glitch of area $A_i^{(+/-)}$, the resultant glitch height is $A_i^{(+/-)}/\tau$. The cut-off frequency ω_c was set to $2\pi f_s/100 = 2\pi\, 10$ krad/s (lower than the Nyquist-frequency $f_s/2$).

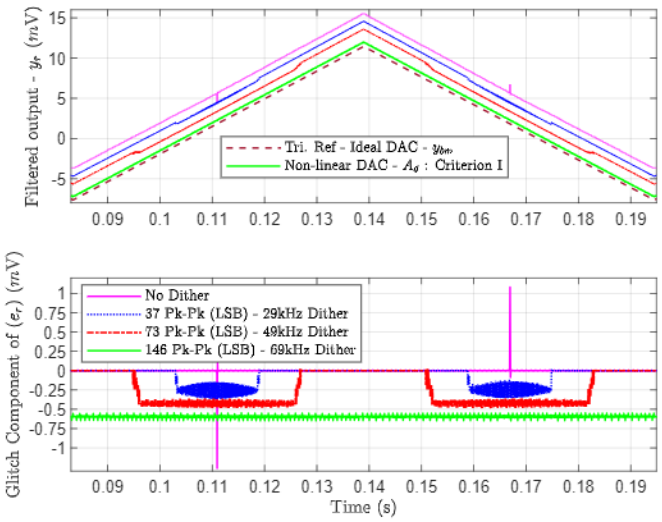

Fig. 7. Dithered glitch response: A) Waveforms of a reconstructed (filtered) 9 Hz, 125 LSB peak-to-peak amplitude triangular wave reference $x(t)$ when using dithers with various frequencies and peak-to-peak amplitudes (plots offset for clarity). B) Isolated glitch-induced error from ideal DAC output.

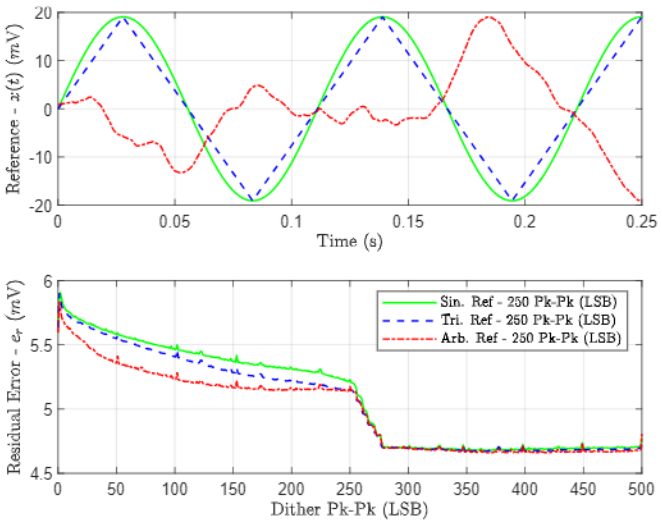

Fig. 8. Illustrating Criterion I: A) Various realisations of $x(t)$ within the range -125–125 LSB; 9 Hz sinusoidal, 9 Hz triangular, and an arbitrary random walk. B) Average residual error e_r dependency on peak-to-peak amplitude of a 49 kHz dither.

B. Results

First consider the equidistant symmetric (minor) glitches n_{g_s} where $\Delta T_s = 1$ LSB and $A_j^+ = -A_j^-$. The dither frequency $1/\rho$ should be chosen within the constraints discussed

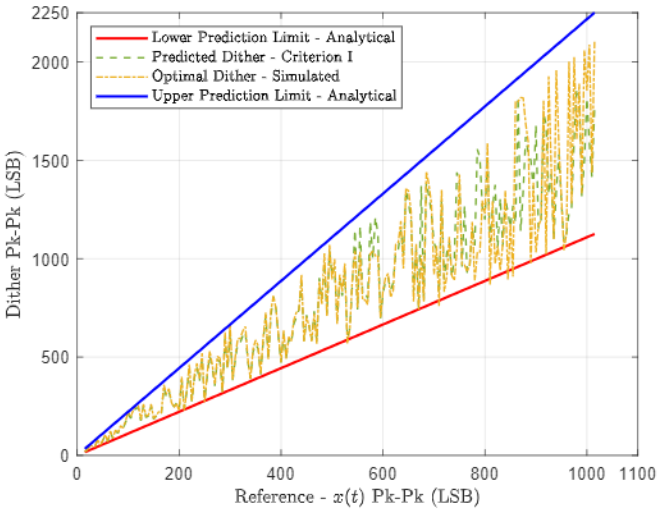

Fig. 9. Validating Criterion I at n_{g_i} for an extended range of random walks at various ranges where $T_i = 0$ LSB is always in the range of $x(t)$. By comparing A_d as predicted in Criterion I due to varying $X_{\min}, X_{\max}$, against A_{optimal} found when seeking the dither amplitude to render $N_i(x)$ constant over the range of x from simulation.

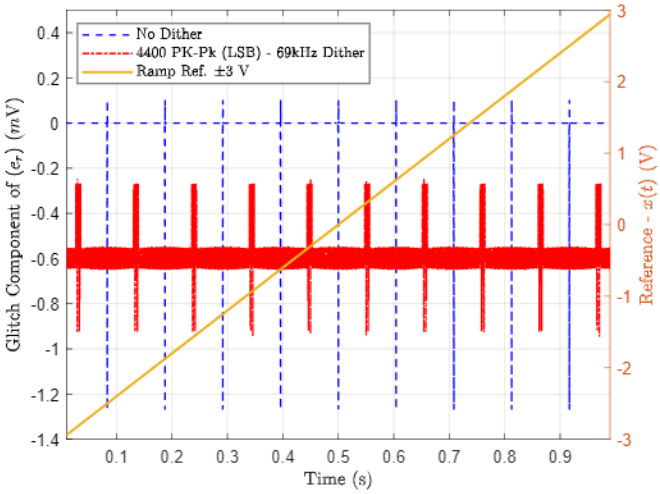

Fig. 10. Illustrating Criterion II: Isolated glitch-induced residual error e_r due to a rising ramp $x(t)$ when A_d is chosen according to Criterion II for a 69 kHz dither.

in Sec. IV, but note from (19) that if

$$\frac{\rho}{\rho - \tau} \approx 1$$

and we choose the dither amplitude $A_d : 2A_d = n\Delta T_s, n \in \mathbb{Z}_{>0}$, then the smoothed non-linearity N_{g_s} can be minimised (i.e., $N_{g_s}(x) = 0$ since $A_j^+ + A_j^- = 0$). This means that the effect of these glitches can be neglected for any dither amplitude that is an integer multiple of the LSB. Hence, we focus on the mitigation of the equidistant major (asymmetric) glitches $n_{g_{\tilde{s}}}$, with $\Delta T_{\tilde{s}} = 4096$ LSB.

The performance is measured by the error between an ideal DAC response, after the smoothing filter, and the response of the validation model. The benchmark response y_{bm} is obtained by bypassing the DAC model; referring to the diagram in Fig. 2, this means setting $\tilde{y} = x$. The smoothing filter is included in the benchmark response to account for the phase lag of this filter. The response error e_r due to the model (30) is then $e_r = y_r - y_{bm}$. The error e_r measures the effect of quantization q, element mismatch n_{em} and glitches n_g, after averaging.

Fig. 7 shows the effect of a single major glitch, without dithering, as well as when applying dithers with different frequencies and amplitudes. In this case, the averaged response corresponds closely to the analytical prediction (13). The error e_r due to n_g is shown in Fig. 7-B.

As predicated by (13), note that the effect of progressively increasing A_d is to widen the sector where N_i is (on average) a constant equal to $(A_i^+ + A_i^-)/\rho = -8.6363/\rho$ nV; i.e., $-0.25, -0.423, -0.596$ mV for $1/\rho = 29, 49, 69$ kHz respectively. When A_d is increased to a value that meets Criterion I in (15) then $N_i(x)$ at $T_i = 0$ LSB is constant at -0.596 mV for all $x \in [-62.5, 62.5]$ LSB when $1/\rho = 69$ kHz. The criterion is met when the amplitude is $A_d = \lceil \rho/(\rho - 2\tau) \cdot \max\{|T_i - X_{\min}|, |T_i - X_{\max}|\} \rceil = \lceil 1.16 \cdot \max\{|0 - (-62.5)|, |0 - 62.5|\} \rceil = 73$ LSB; i.e. dither peak-to-peak amplitude $2A_d = 146$ LSB.

The output is not completely constant; there is some ripple. This is explained by (5), where $(x - \tilde{x}) \to 0$ as $\rho \to 0$. The ripple is reduced by increasing the dither frequency, and it can be seen that the ripple is smaller for $1/\rho = 69$ kHz than $1/\rho = 49$ kHz or $1/\rho = 29$ kHz.

As can be seen in Fig. 7, the effective glitch can essentially be converted from an impulse-like disturbance with large amplitude to a constant (with some ripple). It can be noted that a lower cut-off frequency in the smoothing filter reduces the effect of the non-dithered glitch, but also reduces the ripple in the dithered case. In practical terms, this means that by introducing dither the detrimental effect of glitches can be reduced in many applications. As an example, in closed-loop applications, the control bandwidth is not sufficient to attenuate impulse disturbances, but compensating for constant disturbances is feasible by using e.g. integral action [21].

Fig. 8 demonstrates how the error e_r is generally input-dependent; i.e. it depends on the trajectory of the input (e.g. the number of T_i crossings and the input value distribution in the neighbourhood of T_i). Fig. 8-B shows how e_r converges to a constant regardless of the realisation of $x(t)$ over a set range, as long as A_d meets Criterion I. This is in accordance with the results in Sec. IV-B; where Criterion I is shown to render e_r constant over the range of $x(t)$. Note that the error e_r is dependent on the input signal realisation (sinusoidal, triangular, or random walk) for dither amplitudes below the limit in Criterion I, but remains constant for all input signals once the dither amplitude satisfies (15). With $1/\rho = 49$ kHz, we have $A_d = 1.11 \cdot \max\{|0 - (-125)|, |0 - 125|\} = 138.5$ LSB; i.e. $2A_d = 277$ LSB.

Fig. 9 shows the results validating Criterion I by simulation for a large variety of dither and reference signals. The model includes a single major glitch with $T_i = 0$ LSB. The reference signal peak-to-peak amplitude $\Delta X = X_{\max} - X_{\min}$ was increased starting from $\Delta X = 15$ LSB up to

$\Delta X = 1015$ LSB such that $T_i \in (X_{\min}, X_{\max})$. For a given $\Delta X(j)$ at simulation run j, a suitable random walk $x(t)$ was generated, similar to the one shown in Fig. 8-A. $A_d(j)$ from Criterion I was predicted at run j given the fixed $X_{\min}(j), X_{\max}(j)$. Then the dither amplitude was gradually increased producing a result similar to Fig. 8-B. Then the smallest amplitude $A_{\text{optimal}}(j)$ to render e_r constant from the simulation was selected for each run j. The predicted A_d from (15) and simulated A_{optimal} amplitudes are compared to each other in Fig. 9. The analytical prediction and verification via simulation correspond well; for all T_i in the range of $x(t)$, the smallest dither amplitude to render e_r constant is bound between $\Delta X/2$ (lower prediction limit) and ΔX (upper prediction limit). Not all simulated results fall between the predicted limits, but this is likely due to using an analytical model that is a simplification of the validation model.

Fig. 10 shows an example for the case of several, equidistant glitches, where the dither amplitude meets Criterion II for a dither frequency of $1/\rho = 69$ kHz. Here $A_d = 1.07411 \cdot \Delta T_{\tilde{s}}/2$; i.e. dither peak-to-peak amplitude is $2A_d = 4400$ LSB. Note that the input is a rising ramp where $x(t) \in [-3, +3]$ V, 60% of FSR. For the non-dithered case, only rising glitches are therefore excited. The number of major glitches to be excited by $x(t)$ is $\lfloor 60\% \times N_{T_{\tilde{s}}} \rfloor = 9$. For the dithered case there are sections with a larger amplitude between consecutive glitches T_i. These are in accordance with (20) and Fig. 5. Note that the filtered glitches (no dither) have the same attenuation observed for the major filtered rising glitch in Fig. 7-B. However, it is noted that the sufficiently dithered glitch at -0.596 mV, has a larger variance around the constant offset compared to what is seen in Fig. 7-B at the same dither frequency; i.e., 69 kHz. This is explained by (5) as L_X for the ramp reference in this case is much larger than that of the 125 LSB peak-to-peak amplitude, 9 Hz triangular reference.

VII. Conclusions

A behavioural analytical model describing glitches was introduced and used to derive criteria for sufficiently large dither amplitudes to mitigate glitches by when using high-frequency periodic dithering and low-pass filtering. The proposed criteria prescribe dither amplitudes where the averaged glitch response becomes a constant over the entire range of operation for the input. The analytical results are validated by a non-linear DAC model with parameters fitted to the measured responses of a commercial DAC. The model includes all significant, observed DAC non-linearities, including glitches. The simulations demonstrate the validity of the analytical results.

References

[1] S. Debnath, J. Qin, B. Bahrani, M. Saeedifard, and P. Barbosa, "Operation, control, and applications of the modular multilevel converter: A review," *IEEE Transactions on Power Electronics*, vol. 30, no. 1, pp. 37–53, 2015.

[2] D. F. Cortez and I. Barbi, "A three-phase multilevel hybrid switched-capacitor pwm pfc rectifier for high-voltage-gain applications," *IEEE Transactions on Power Electronics*, vol. 31, no. 5, pp. 3495–3505, 2016.

[3] C. Zhang, M. Takongmo, S. Wdaan, W. A. M. Telmesani, D. Yapa, and J. Salmon, "Carrier transition techniques for parallel connected vscs using cross-coupled inductors," *IEEE Transactions on Power Electronics*, vol. 37, no. 8, pp. 9652–9662, 2022.

[4] B. Armstrong-Hélouvry, P. Dupont, and C. C. De Wit, "A survey of models, analysis tools and compensation methods for the control of machines with friction," *Automatica*, vol. 30, no. 7, pp. 1083–1138, 1994.

[5] Z. Jamaludin, H. Van Brussel, and J. Swevers, "Quadrant glitch compensation using friction model-based feedforward and an inverse-model-based disturbance observer," in *2008 10th IEEE International Workshop on Advanced Motion Control*. IEEE, 2008, pp. 212–217.

[6] P. Hendriks, "Specifying Communications DACs," *IEEE Spectrum*, vol. 34, no. 7, pp. 58–69, jul 1997.

[7] R. J. van de Plassche, *CMOS Integrated Analog-to-Digital and Digital-to-Analog Converters*. Kluwer Academic Publishers, 2003.

[8] M. J. Pelgrom, *Analog-to-Digital Conversion*, 2nd ed. Springer-Verlag, 2013.

[9] P. Horowitz and W. Hill, *The Art of Electronics*, 3rd ed. Cambridge University Press, 2015.

[10] W. Kester and A. D. I. Engineeri, *Data conversion handbook*. Newnes, 2005.

[11] K. Andersson and M. Vesterbacka, "Modeling of Glitches Due to Rise/fall Asymmetry in Current-steering Digital-to-analog Converters," *IEEE Trans. Circuits Syst. I*, vol. 52, no. 11, pp. 2265–2275, 2005.

[12] R. A. Wannamaker, S. Lipshitz, J. Vanderkooy, and J. N. Wright, "A Theory of Nonsubtractive Dither," *IEEE Trans. Signal Process.*, vol. 48, no. 2, pp. 499–516, 2000.

[13] B. Widrow and I. Kollár, *Quantization Noise*. Cambridge University Press, 2008.

[14] A. A. Eielsen and A. J. Fleming, "Improving Digital-to-Analog Converter Linearity by Large High-Frequency Dithering," *IEEE Trans. Circuits Syst. I*, vol. 64, no. 6, pp. 1409–1420, 2017.

[15] C. A. Desoer and S. M. Shahruz, "Stability of dithered non-linear systems with backlash or hysteresis," *International Journal of Control*, vol. 43, no. 4, pp. 1045–1060, 1986.

[16] A. A. Eielsen, J. Leth, A. J. Fleming, A. G. Wills, and B. Ninness, "Large-amplitude dithering mitigates glitches in digital-to-analogue converters," *IEEE Transactions on Signal Processing*, vol. 68, pp. 1950–1963, 2020.

[17] R. Oldenburger and R. C. Boyer, "Effects of Extra Sinusoidal Inputs to Nonlinear Systems," *J Basic Eng-T ASME*, vol. 84, no. 4, pp. 559–569, 1962.

[18] G. Zames and N. A. Shneydor, "Dither in Nonlinear Systems," *IEEE Trans. Autom. Control*, vol. 21, no. 5, pp. 660–667, 1976.

[19] S. Mossaheb, "Application of a method of averaging to the study of dithers in non-linear systems," *Int J Control*, vol. 38, no. 3, pp. 557–576, 1983.

[20] L. Iannelli, K. H. Johansson, U. T. Jönsson, and F. Vasca, "Averaging of nonsmooth systems using dither," *Automatica*, vol. 42, no. 4, pp. 669–676, 2006.

[21] A. Faza', A. A. Eielsen, and J. Leth, "Mitigating non-linear dac glitches using dither in closed-loop nano-positioning applications," in *2023 American Control Conference (ACC)*. IEEE, 2022, (in press).

[22] G. C. Goodwin, S. F. Graebe, and M. E. Salgado, *Control System Design*. Prentice Hall, Inc., 2000.